We are IntechOpen, the world's leading publisher of Open Access books Built by scientists, for scientists

6,900
Open access books available

185,000
International authors and editors

200M
Downloads

Our authors are among the

154
Countries delivered to

TOP 1%
most cited scientists

12.2%
Contributors from top 500 universities



WEB OF SCIENCE™

Selection of our books indexed in the Book Citation Index in Web of Science™ Core Collection (BKCI)

Interested in publishing with us?
Contact book.department@intechopen.com

Numbers displayed above are based on latest data collected.
For more information visit www.intechopen.com



17

Biometrics Sensor Fusion

Dakshina Ranjan Kisku, Ajita Rattani, Phalguni Gupta,
Jamuna Kanta Sing and Massimo Tistarelli
Dr. B. C. Roy Engineering College, Durgapur – 713206, India
University of Sassari, Alghero (SS), 07140, Italy
Indian Institute of Technology Kanpur, Kanpur – 208016, India
Jadavpur University, Kolkata – 700032, India
University of Sassari, Alghero (SS), 07140, Italy

1. Introduction

Performance of any biometric system entirely depends on the information that is acquired from biometrics characteristics (Jain et. al., 2004). Several biometrics systems are developed over the years in the last two decades, which are mostly considered as viable biometric tools used for human identification and verification. However, due to some negative constraints that are often associated with the biometrics templates are generally degraded the overall performance and accuracy of the biometric systems. In spite of that, many biometrics systems are developed and implemented over the years and deployed successfully for user authentication. Modality based categorization of the biometric systems are made on the basis of biometric traits are used. While single biometric systems are used for verification or identification of acquired biometrics characteristics/attributes, it is called uni-biometrics authentication systems and when more than one biometric technology are used in fused form for identification or verification, it is called multimodal biometrics. It has been seen that, depending on the application context, mono-modal or multimodal biometrics systems can be used for authentication.

In biometric, human identity verification systems seek considerable improvement in reliability and accuracy. Several biometric authentication traits are offering 'up-to-the-mark' and negotiable performance in respect of recognizing and identifying users. However, none of the biometrics is giving cent percent accuracy. Multibiometric systems remove some of the drawbacks of the uni-modal biometric systems by acquiring multiple sources of information together in an augmented group, which has richer details. Utilization of these biometric systems depends on more than one physiological or behavioral characteristic for enrollment and verification/ identification. There exist multimodal biometrics (Jain et. al., 2004) with various levels of fusion, namely, sensor level, feature level, matching score level and decision level. Further, fusion at low level / sensor level by biometric image fusion is an emerging area of research for biometric authentication.

A multisensor multimodal biometric system fuses information at low level or sensor level of processing is expected to produce more accurate results than the systems that integrate

information at a later stages, namely, feature level, matching score level, because of the availability of more richer and relevant information.
Face and palmprint biometrics have been considered and accepted as most widely used biometric traits, although the fusion of face and palmprint is not studied at sensor level/low level when it is compared with existing multimodal biometric fusion schemes. Due to incompatible characteristics of face and palmprint images, where a face image is processed as holistic texture features on a whole face or divided the face into local regions and palmprint consists of ridges and bifurcations along with three principal lines, difficult to integrate in different levels of fusion in biometric.
This chapter proposes a novel biometric sensor generated evidence fusion of face and palmprint images using wavelet decomposition and monotonic decreasing graph for user identity verification. Biometric image fusion at sensor level refers to a process that fuses multispectral images captured at different resolutions and by different biometric sensors to acquire richer and complementary information to produce a fused image in spatially enhanced form. SIFT operator is applied for invariant feature extraction from the fused image and the recognition of individuals is performed by adjustable structural graph matching between a pair of fused images by searching corresponding points using recursive descent tree traversal approach. The experimental results show that the proposed method with 98.19% accuracy is found to be better than the uni-modal face and palmprint authentication having recognition rates 89.04% and 92.17%, respectively if all methods are processed in the same feature space, i.e., in SIFT feature space.
The chapter is organized as follows. Next section introduces a few state-of-the-art biometrics sensor fusion methods for user authentication and recognition. Section 3 discusses the process of multisensor biometric evidence fusion using wavelet decomposition and transformation. Section 4 presents the overview of feature extraction by using SIFT features from fused image. Structural graph for corresponding points searching and matching is analyzed in Section 5. Experimental results are discussed in section 6 and conclusion is drawn in the last section.

2. State-of-the-art Biometrics Sensor Fusion Methods

In this section two robust multisensor biometrics methods are discussed briefly for user authentication. The first method (Raghavendra, et. al., 2010) has presented a novel biometric sensor fusion technique for face and palmprint images using Particle Swarm Optimisation (PSO). The method consists of the following steps. First the face and palmprint images obtained from different sensors are decomposed using wavelet transformation and then, PSO is employed to select the most discriminative wavelet coefficients from face and palmprint to produce a new fused image. Kernel Direct Discriminant Analysis (KDDA) has been applied for feature extraction and the decision about accept/reject is carried out using Nearest Neighbour Classifier. (NNC).
The second method (Singh, et. al., 2008) is a multispectral image fusion of visible and infrared face images and verification decision is made using match score fusion. The fusion of visible and long wave infrared face images is performed using 2vn-granular SVM which uses multiple SVMs to learn both the local and global properties of the multispectral face images at different granularity levels and resolution. The 2vn-GSVM performs accurate classification which is subsequently used to dynamically compute the weights of visible and

infrared images for generating a fused face image. 2D log polar Gabor transform and local binary pattern feature extraction algorithms are applied to the fused face image to extract global and local facial features, respectively. The corresponding matching scores are fused using Dezert Smarandache theory of fusion which is based on plausible and paradoxical reasoning. The efficacy of the proposed algorithm is validated using the Notre Dame and Equinox databases and is compared with existing statistical, learning, and evidence theory based fusion algorithms.

3. Multisensor Biometrics Evidence Fusion using Wavelet Decomposition

Multisensor image fusion is performed with one or more images; however the fused image is considered as a unique single pattern from where the invariant keypoint features are extracted. The fused image should have more useful and richer information together from individual images. The fusion of the two images can take place at the signal, pixel, or feature level.

The proposed method for evidence fusion is based on the face and palmprint images decomposition into multiple channels depending on their local frequency. The wavelet transform provides an integrated framework to decompose biometric images into a number of new images, each of them having a different degree of resolution. According to Fourier transform, the wave representation is an intermediate representation between Fourier and spatial representations. It has the capability to provide good optimal localization for both frequency and space domains.

3.1 Basic Structure for Image Fusion

The biometrics image fusion extracts information from each source image and obtains the effective representation in the final fused image. The aim of image fusion technique is to fuse the detailed information which obtains from both the source images. By convention, multi-resolutions images are used for image fusion, which are obtained from different sources. Multi-resolution analysis of images provides useful information for several computer vision and image analysis applications. The multi-resolution image used to represent the signals where decomposition is performed for obtaining finer detail. Multi-resolution image decomposition gives an approximation image and three other images viz., horizontal, vertical and diagonal images of coarse detail. The Multi-resolution techniques are mostly used for image fusion using wavelet transform and decomposition.

Our method proposes a scheme where we fuse biometrics face and palmprint images of the identical resolutions and the images are completely different in texture information. The face and palmprint images are obtained from different sources. More formally, these images are obtained from different sensors. After re-scaling and registration, the images are fused together by using wavelet transform and decomposition. Finally, we obtain a completely new fused image, where both the attributes of face and palmprint images are focused and reflected. The proposed method for image fusion opposes the multi-resolution image fusion approach where multi-resolution images of same the subject are collected from multiple sources. However, these multi-resolution images belong to the same subject rather than different subjects. In the proposed approach, face and palmprint images are acquired from two different sensors, i.e., from two different sources and to make alignment of the corresponding pixels, feature-based image registration algorithm has been used (Hsu, & Beuker, 2000).

Prior to image fusion, wavelet transforms are determined from face and palmprint images. The wavelet transform contains low-high bands, high-low bands and high-high bands of the face and palmprint images at different scales including the low-low bands of the images at coarse level. The low-low band has all the positive transform values and remaining bands have transform values which are fluctuating around zeros. The larger transform values in these bands respond to sharper brightness changes and thus to the changes of salient features in the image such as edges, lines, and boundaries. The proposed image fusion rule selects the larger absolute values of the two wavelet coefficients at each point. Therefore, a fused image is produced by performing an inverse wavelet transform based on integration of wavelet coefficients correspond to the decomposed face and palmprint images. More formally, wavelet transform decomposes an image recursively into several frequency levels and each level contains transform values. Let it be a gray-scale image, after wavelet decomposition, the first level would be

$$I = I_{LL_1} + I_{LH_1} + I_{HL_1} + I_{HH_1} \tag{1}$$

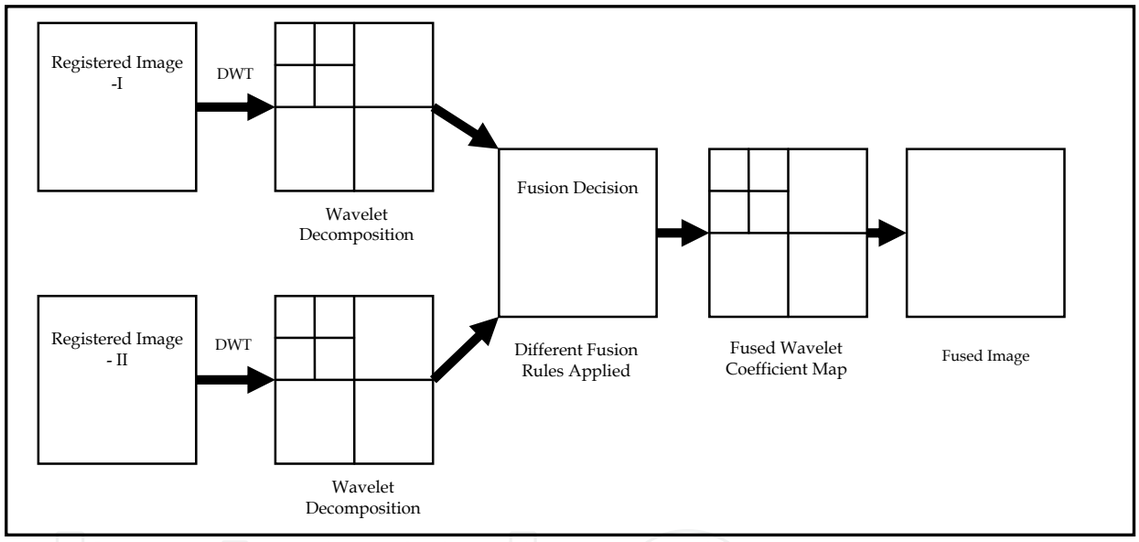


Fig. 1. Generic structure of wavelet based fusion approach.

Generally, I_{LL_1} represents the base image, which contains coarse detail of positive transform values and the other high frequency detail such as I_{LH_1}, I_{HL_1} and I_{HH_1} represent the vertical, horizontal and diagonal detail of transform values, respectively, and these details fluctuating transform values around zeros. After nth level decomposition of the base image in low frequency, the nth level would be the following:

$$I_{n-1} = I_{LL_n} + I_{LH_n} + I_{HL_n} + I_{HH_n} \tag{2}$$

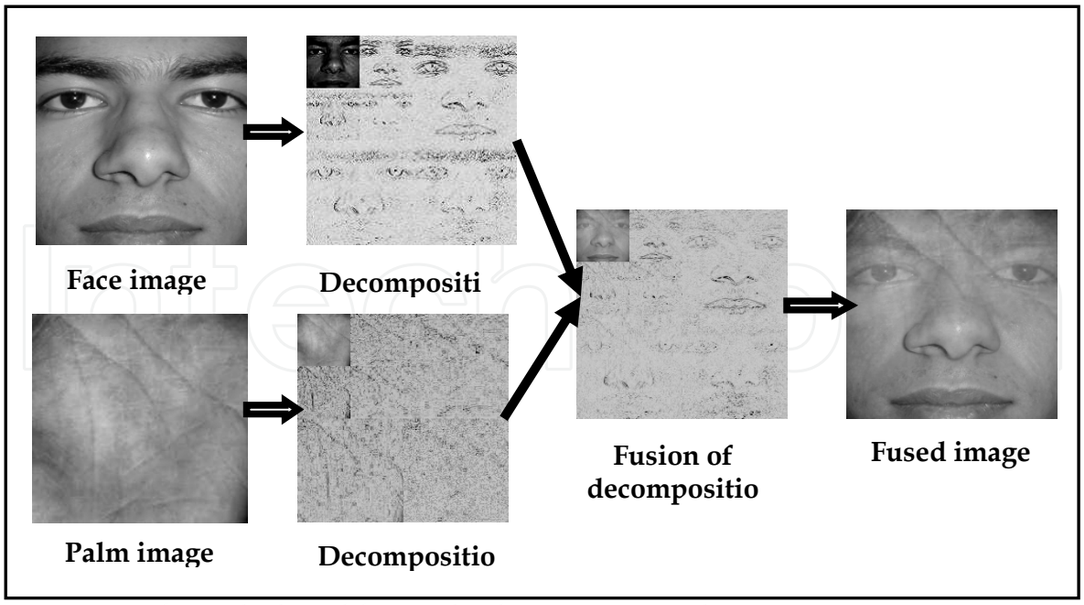


Fig. 2. Fusion of wavelet based face and palmprint images decompositions.

So, the nth level of decomposition will be consisting of 3n+1 sub-image sequences. The 3n+1 sub-image sequences are then fused by applying different wavelet fusion rules on the low and high frequency parts. Finally, inverse wavelet transformation is performed to restore the fused image. The fused image possesses good quality of relevant information for face and palm images. Generic wavelet-based decomposition and image fusion approach are shown in the Fig. 1 and Fig. 2 respectively.

4. SIFT Features Extraction

To recognize and classify objects efficiently, feature points from objects can be extracted to make a robust feature descriptor or representation of the objects. In this work the technique to extract features from images, which are called Scale Invariant Feature Transform (SIFT) (Lowe, 2004; Lowe, 1999) has been used. These features are invariant to scale, rotation, partial illumination and 3D projective transform and they are found to provide robust matching across a substantial range of affine distortion, change in 3D viewpoint, addition of noise, and change in illumination. SIFT image features provide a set of features of an object that are not affected by occlusion, clutter, and unwanted "noise" in the image. In addition, the SIFT features are highly distinctive in nature which have accomplished correct matching on several pair of feature points with high probability between a large database and a test sample. Following are the four major filtering stages of computation used to generate the set of image feature based on SIFT.

4.1 Scale-space Extrema Detection

This filtering approach attempts to identify image locations and scales that are identifiable from different views. Scale space and Difference of Gaussian (DoG) functions are used to detect stable keypoints. Difference of Gaussian is used for identifying key-points in scale-space and locating scale space extrema by taking difference between two images, one with

scaled by some constant times of the other. To detect the local maxima and minima, each feature point is compared with its 8 neighbors at the same scale and in accordance with its 9 neighbors up and down by one scale. If this value is the minimum or maximum of all these points then this point is an extrema. More formally, if a DoG image is given as *D(x, y, σ)*, then

$$D(x, y, \sigma) = L(x, y, k_i\sigma) - L(x, y, k_j\sigma) \quad (3)$$

where *L(x, y, kσ)* is the convolution of the original image *I(x, y)* with the Gaussian blur *G(x, y, kσ)* at scale *kσ*, i.e.,

$$L(x, y, k\sigma) = G(x, y, k\sigma) * I(x, y) \quad (4)$$

where * is the convolution operator in x and y, and

$$G(x, y, \sigma) = \frac{1}{2\pi\sigma^2} e^{-(x^2+y^2)/2\sigma^2}$$

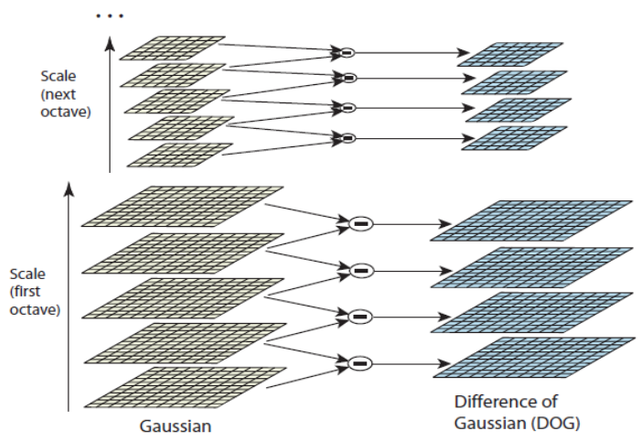


Fig. 3. Difference-of-Gaussian (DoG) octave (Lowe, 1999).

From Equations (3) and (4) it can be concluded that a *DoG* image between scales $k_i\sigma$ and $k_j\sigma$ is just the difference of the Gaussian-blurred images at scales $k_i\sigma$ and $k_j\sigma$. For scale-space extrema detection with the SIFT algorithm, the image is first convolved with Gaussian-blurs at different scales. The convolved images are grouped by octave (an octave corresponds to doubling the value of σ), and the value of k_i is selected so that we obtain a fixed number of convolved images per octave. Then the Difference-of-Gaussian images are taken from adjacent Gaussian-blurred images per octave. Fig. 3 shows difference-of-gaussian octave.

4.2 Keypoints Localization

To localize keypoints, a few points after detection of stable keypoint locations that have low contrast or are poorly localized on an edge are eliminated. This can be achieved by calculating the Laplacian space. After computing the location of extremum value, if the

value of difference of Gaussian pyramids is less than a threshold value the point is excluded. If there is a case of large principle curvature across the edge but a small curvature in the perpendicular direction in the difference of Gaussian function, the poor extrema is localized and eliminated.

First, for each candidate keypoint, interpolation of nearby data is used to accurately determine its position. The initial approach is to just locate each keypoint at the location and scale of the candidate keypoint while the new approach calculates the interpolated location of the extremum, which substantially improves matching and stability. The interpolation is done using the quadratic expansion of the Difference-of-Gaussian scale-space function, $D(x, y, \sigma)$ with the candidate keypoint as the origin. This Taylor expansion is given by:

$$D(p) = D + \frac{\partial D^T}{\partial p} p + \frac{1}{2} p^T \frac{\partial^2 D}{\partial p^2} p \tag{5}$$

where D and its derivatives are evaluated at the sample point and $p = (x, y, \sigma)^T$ is the offset from this point. The location of the extremum, $\hat{p}$ is determined by taking the derivative of this function with respect to p and setting it to zero, giving

$$\hat{x} = -\frac{\partial^2 D^{-1}}{\partial x^2} \frac{\partial D}{\partial x} \tag{6}$$

If the offset p is larger than 0.5 in any dimension, then it is an indication that the extremum lies closer to another candidate keypoint. In this case, the candidate keypoint is changed and the interpolation performed instead about that point. Otherwise the offset is added to its candidate keypoint to get the interpolated estimate for the location of the extremum.

4.3 Assign Keypoints Orientation

This step aims to assign consistent orientation to the key-points based on local image characteristics. From the gradient orientations of sample points, an orientation histogram is formed within a region around the key-point. Orientation assignment is followed by key-point descriptor which can be represented relative to this orientation. A 16x16 window is chosen to generate histogram. The orientation histogram has 36 bins covering 360 degree range of orientations. The gradient magnitude and the orientation are pre-computed using pixel differences. Each sample is weighted by its gradient magnitude and by a Gaussian-weighted circular window.

Following experimentation with a number of approaches to assign a local orientation, the following approach has been found to give the most stable results. The scale of the keypoint is used to select the Gaussian smoothed image, L, with the closest scale, so that all computations are performed in a scale-invariant manner. For each image sample, $L(x, y)$, at this scale, the gradient magnitude, $m(x, y)$, and orientation, $\theta(x, y)$, is precomputed using pixel differences:

$$m(x, y) = \sqrt{(L(x+1, y) - L(x-1, y))^2 + (L(x, y+1) - L(x, y-1))^2} \tag{7}$$

$$\Theta(x, y) = \tan^{-1}\left(\left(L(x, y+1) - L(x, y-1)\right) / \left(L(x+1, y) - L(x-1, y)\right)\right) \quad (8)$$

An orientation histogram is formed from the gradient orientations of sample points within a region around the keypoint. The orientation histogram has 36 bins covering the 360 degree range of orientations. Each sample added to the histogram is weighted by its gradient magnitude and by a Gaussian-weighted circular window with a σ that is 1.5 times that of the scale of the keypoint.

4.4 Generation of Keypoints Descriptor

In the last step, the feature descriptors which represent local shape distortions and illumination changes are computed. After candidate locations have been found, a detailed fitting is performed to the nearby data for the location, edge response and peak magnitude. To achieve invariance to image rotation, a consistent orientation is assigned to each feature point based on local image properties. The histogram of orientations is formed from the gradient orientation at all sample points within a circular window of a feature point. Peaks in this histogram correspond to the dominant directions of each feature point. For illumination invariance, 8 orientation planes are defined. Finally, the gradient magnitude and the orientation are smoothened by applying a Gaussian filter and then are sampled over a 4 x 4 grid with 8 orientation planes. Keyppoint descriptor generation is shown in Fig. 4.

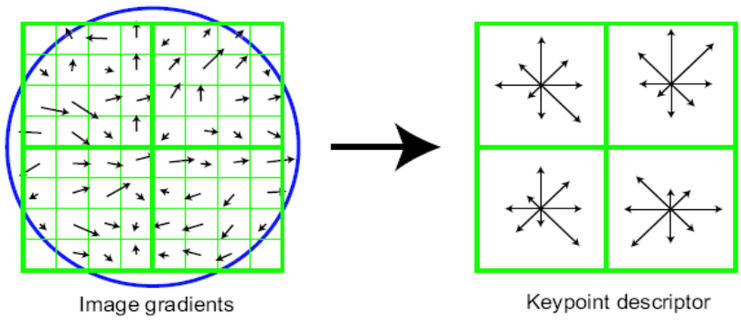


Fig. 4. A keypoint descriptor created by the gradient magnitude and the orientation at each point in a region around the keypoint location.

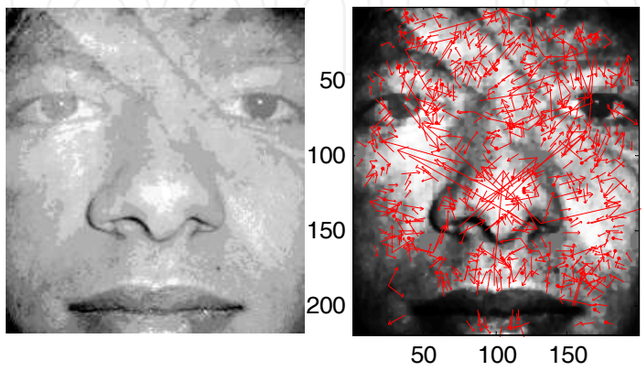


Fig. 5. Fig. 5(a) Fused Image, (b) Fused Image with extracted SIFT features.

In the proposed work, the fused image is normalized by histogram equalization and after normalization invariants SIFT features are extracted from the fused image. Each feature point is composed of four types of information – spatial location (*x*, *y*), scale (*S*), orientation (θ) and Keypoint descriptor (*K*). For the sake experiment, only keypoint descriptor information has been taken which consists of a vector of 128 elements representing neighborhood intensity changes of current points. More formally, local image gradients are measured at the selected scale in the region around each keypoint. The measured gradients information is then transformed into a vector representation that contains a vector of 128 elements for each keypoints calculated over extracted keypoints. These keypoint descriptor vectors represent local shape distortions and illumination changes. In Fig. 5, SIFT features extracted on the fused image are shown.
Next section discusses the matching technique by structural graph for establishing correspondence between a pair of fused biometric images by searching a pair of point sets using recursive descent tree traversal algorithm (Cheng, et. al., 1991).

5. Matching using Monotonic-Decreasing Graph

In order to establish a monotonic-decreasing graph based relation (Lin, et. al., 1986; Cheng, et. al., 1988) between a pair of fused images, a recursive approach based tree traversal algorithm is used for searching the feature points on the probe/query fused sample, which are corresponding to the points on the database/gallery fused sample. Verification is performed by computing of differences between a pair of edges that are members of original graph on gallery sample and graph on probe sample, respectively.
The basic assumption is that the moving features points are rigid. Let $\{g_1, g_2, ..., g_m\}$ and $\{p_1, p_2, ..., p_n\}$ be two sets of feature points at the two time instances where *m* and *n* may or may not be same. Generally, identical set of feature points are not available from a pair of instances of a same user or from different users. So, It is assumed that $m \neq n$.
The method is based on the principle of invariance of distance measures under rigid body motion where deformation of objects does not occur. Using the strategy in [8], maximal matching points and minimum matching error obtained. First, we choose a set of three points, say g_1, g_2 and g_3 on a given fused gallery image which are uniquely determined. By connecting these points with each other we form a triangle $\Delta g_1 g_2 g_3$ and three distances, $d(g_1, g_2), d(g_2, g_3)$ and $d(g_1, g_3)$ are computed. Now, we try to locate another set of three points, p_i, p_j and p_k on a given fused probe image that also form a triangle that would be best matching the triangle $\Delta g_1 g_2 g_3$. Best match would be possible when the edge (p_i, p_j) matches the edge (g_1, g_2), (p_j, p_k) matches (g_2, g_3) and (p_i, p_k) matches (g_1, g_3). This can be attained when these matches lie within a threshold ε. We can write,

$$\begin{cases} |\, d(p_i, p_j) - d(g_1, g_2) \,| \leq \varepsilon_1 \\ |\, d(p_j, p_k) - d(g_2, g_3) \,| \leq \varepsilon_2 \\ |\, d(p_i, p_k) - d(g_1, g_3) \,| \leq \varepsilon_3 \end{cases} \tag{9}$$

Equation (9) is used for making closeness between a pair of edges using edge threshold ε. Traversal would be possible when p_i correspond to g_1 and p_j corresponds to g_2 or conversely, p_j to g_1 and p_i to g_2. Traversal can be initiated from the first edge (p_i, p_j) and by visiting n feature points, we can generate a matching graph $P' = (p_1', p_2', p_3', ..., p_m')$ on the fused probe image which should be a corresponding candidate graph of G. In each recursive traversal, a new candidate graph P_i' is found. At the end of the traversal algorithm, a set of candidate graphs $P_i' = (p_{1i}', p_{2i}', p_{3i}', ..., p_{mi}')$ i = 1,2,…,m is found and all of which are having identical number of feature points.

For illustration, consider the minimal k^{th} order error from $G.$, the final optimal graph P'' can be found from the set of candidate graphs P_i' and we can write,

$$| P'' - G |_k \leq | P_i' - G |_k, \forall i \tag{10}$$

The k^{th} order error between P'' and G can be defined as

$$| P'' - G |_k = \sum_{i=2}^{m} \sum_{j=1}^{\min(k, i-1)} | d(p_i', p_{i-j}') - d(g_i, g_{i-j}) |, \tag{11}$$
$$\forall k, k = 1,2,3,..., m$$

The Equation (11) denotes sum of all differences between a pair edges corresponding to a pair of graphs. This sum can be treated as final dissimilarity value for a pair of graphs and also for a pair of fused images. It is observed that, when k is large, the less error correspondence is found. This is not always true as long as we have a good choice of the edge threshold ϵ. Although for the larger k, more comparison is needed. For identity verification of a person, client-specific threshold has been determined heuristically for each user and the final dissimilarity value is then compared with client-specific threshold and decision is made.

6. Experiment Results

The experiment is carried out on multimodal database of face and palmprint images collected at IIT Kanpur which consists of 750 face images and 750 palmprint images of 150 individuals. Face images are captured under control environment with $\pm 20^0$ changes of head pose and with at most uniform lighting and illumination conditions and with almost consistent facial expressions. For the sake of experiment, cropped frontal view face has been taken covering face portion only. For the palmprint database, cropped palm portion has been taken from each palmprint image which contains three principal lines, ridges and bifurcations. The proposed multisensor biometric evidence fusion method is considered as a semi-sensor fusion approach with some minor adjustable corrections in terms of cropping and registration. Biometric sensors generated face and palmprint images are fused at low level by using wavelet decomposition and fusion of decompositions. After fusion of

cropped face and palmprint images of 200×220 pixels, the resolution for fused image has been set to 72 dpi. The fused image is then pre-processed by using histogram equalization. Finally, the matching is performed between a pair of fused images by structural graphs drawn on both the gallery and the probe fused images using extracted SIFT keypoints.

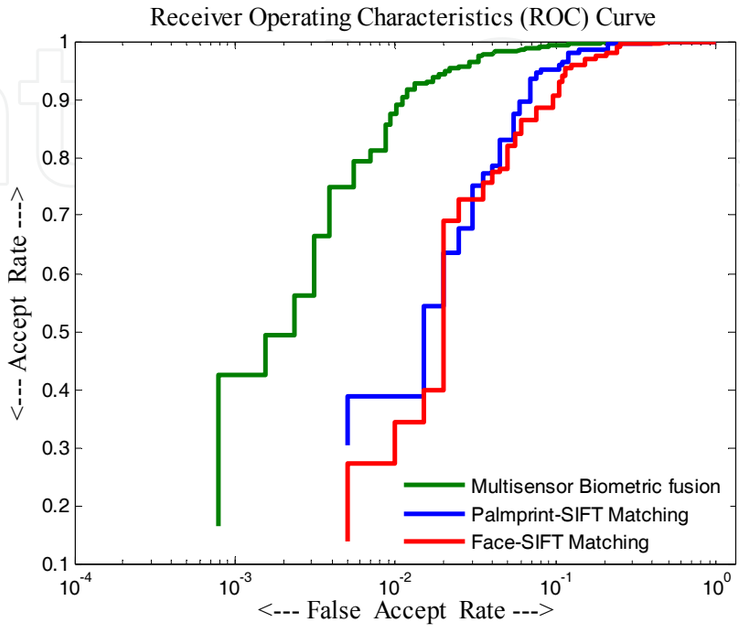


Fig. 6. ROC curves (in 'stairs' form) for the different methods.

The matching is accomplished for the method and the results show that fusion performance at the semi-sensor level / low level is found to be superior when it is compared with two monomodal methods, namely, palmprint verification and face recognition drawn on same feature space. Multisensor biometric fusion produces 98.19% accuracy while face recognition and palmprint recognition systems produce 89.04% accuracy and 92.17% accuracy respectively, as shown in the Fig. 6. ROC curves shown in Figure 6 illustrate the trade-off between accept rate and false accept rate. Further, it shows that the increase in accept rate accompanied by decrease in false accept rate happens in each modality, namely, multisensor biometric evidence fusion, palmprint matching and face matching.

7. Conclusion

A novel and efficient method of multisensor biometric image fusion of face and palmprint for personal authentication has been presented in this chapter. High-resolution multisensor face and palmprint images are fused using wavelet decomposition process and matching is performed by monotonic-decreasing graph drawn on invariant SIFT features. For matching, correspondence has been established by searching feature points on a pair of fused images using recursive approach based tree traversal algorithm. To verify the identity of a person, test has been performed with IITK multimodal database consisting of face and palmprint samples. The result shows that the proposed method initiated at the low level / semi-sensor level is robust, computationally efficient and less sensitive to unwanted noise confirming the

validity and efficacy of the system, when it is compared with mono-modal biometric recognition systems.

8. References

Bicego, M., Lagorio, A., Grosso, E. & Tistarelli, M. (2006). On the use of SIFT features for face authentication. *Proceedings of International Workshop on Biometrics, in association with CVPR*.

Cheng, J-C. & Don, H-S. (1991). *A graph matching approach to 3-D point correspondences*

Cheng, J.C. & Dong Lee, H.S. (1988). A Structural Approach to finding the point correspondences between two frames. *Proceedings of International Conference on Robotics and Automation*, pp. 1810 -1815.

Hsu, C. & Beuker, R. (2000). Multiresolution feature-based image registration. *Proceedings of the Visual Communications and Image Processing,* pp. 1 – 9.

http://www.eecs.lehigh.edu/SPCRL/IF/image_fusion.htm

Jain, A.K. & Ross, A. (2004). Multibiometric systems. *Communications of the ACM*, vol. 47, no.1, pp. 34 - 40.

Jain, A.K., Ross, A. & Pankanti, S. (2006). Biometrics: A tool for information security. *IEEE Transactions on Information Forensics and Security*, vol. 1, no. 2, pp. 125 – 143.

Jain, A.K., Ross, A. & Prabhakar, S. (2004). An introduction to biometrics recognition. *IEEE Transactions on Circuits and Systems for Video Technology*, vol. 14, no. 1, pp. 4 – 20.

Lin, Z.C., Lee, H. & Huang, T.S. (1986). Finding 3-D point correspondences in motion estimation. *Proceeding of International Conference on Pattern Recognition*, pp.303 – 305.

Lowe, D. G. (2004). Distinctive image features from scale invariant keypoints. *International Journal of Computer Vision*, vol. 60, no. 2.

Lowe, D.G. (1999). Object recognition from localscale invariant features. *International Conference on Computer Vision*, pp. 1150 – 1157.

Park, U., Pankanti, S. & Jain, A.K. (2008). Fingerprint Verification Using SIFT Features. *Proceedings of SPIE Defense and Security Symposium*.

Poh, N., & Kittler, J. (2008). On Using Error Bounds to Optimize Cost-sensitive Multimodal Biometric Authentication. *17th International Conference on Pattern Recognition,* pp. 1 – 4.

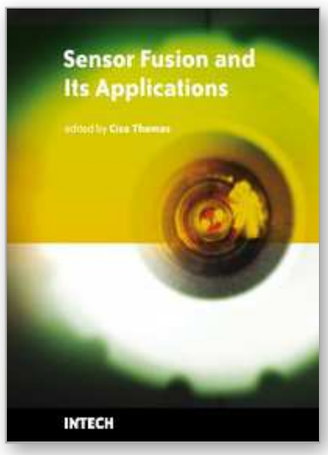
Raghavendra, R., Rao, A. & Kumar, G.H. (2010). Multisensor biometric evidence fusion of face and palmprint for person authentication using Particle Swarm Optimization (PSO). *International Journal of Biometrics (IJBM),* Vol. 2, No. 1.

Ross, A. & Govindarajan, R. (2005). Feature Level Fusion Using Hand and Face Biometrics. *Proceedings of SPIE Conference on Biometric Technology for Human Identification II*, pp. 196 – 204.

Ross, A. & Jain, A.K. (2003). Information Fusion in Biometrics. *Pattern Recognition Letters*, vol. 24, pp. 2115 – 2125.

Singh, R., Vatsa, M. & Noore, A. (2008). Integrated Multilevel Image Fusion and Match Score Fusion of Visible and Infrared Face Images for Robust Face Recognition. *Pattern Recognition - Special Issue on Multimodal Biometrics*, Vol. 41, No. 3, pp. 880-893.

Stathaki, T. (2008). *Image Fusion – Algorithms and Applications.* Academic Press, U.K.



Sensor Fusion and its Applications

Edited by Ciza Thomas

ISBN 978-953-307-101-5

Hard cover, 488 pages

Publisher Sciyo

Published online 16, August, 2010

Published in print edition August, 2010

This book aims to explore the latest practices and research works in the area of sensor fusion. The book intends to provide a collection of novel ideas, theories, and solutions related to the research areas in the field of sensor fusion. This book is a unique, comprehensive, and up-to-date resource for sensor fusion systems designers. This book is appropriate for use as an upper division undergraduate or graduate level text book. It should also be of interest to researchers, who need to process and interpret the sensor data in most scientific and engineering fields. The initial chapters in this book provide a general overview of sensor fusion. The later chapters focus mostly on the applications of sensor fusion. Much of this work has been published in refereed journals and conference proceedings and these papers have been modified and edited for content and style. With contributions from the world's leading fusion researchers and academicians, this book has 22 chapters covering the fundamental theory and cutting-edge developments that are driving this field.

How to reference

In order to correctly reference this scholarly work, feel free to copy and paste the following:

Dakshina Kisku, Ajita Rattani, Phalguni Gupta, Massimo Tistarelli and Jamuna Kanta Sing (2010). Biometrics Sensor Fusion, Sensor Fusion and its Applications, Ciza Thomas (Ed.), ISBN: 978-953-307-101-5, InTech, Available from: http://www.intechopen.com/books/sensor-fusion-and-its-applications/biometrics-sensor-fusion

INTECH
open science | open minds

InTech Europe

University Campus STeP Ri
Slavka Krautzeka 83/A
51000 Rijeka, Croatia
Phone: +385 (51) 770 447
Fax: +385 (51) 686 166
www.intechopen.com

InTech China

Unit 405, Office Block, Hotel Equatorial Shanghai
No.65, Yan An Road (West), Shanghai, 200040, China
中国上海市延安西路65号上海国际贵都大饭店办公楼405单元
Phone: +86-21-62489820
Fax: +86-21-62489821

© 2010 The Author(s). Licensee IntechOpen. This chapter is distributed under the terms of the Creative Commons Attribution-NonCommercial-ShareAlike-3.0 License, which permits use, distribution and reproduction for non-commercial purposes, provided the original is properly cited and derivative works building on this content are distributed under the same license.

IntechOpen

IntechOpen